Journal of Cerebral Blood Flow & Metabolism (2010) 30, 1608–1618

www.jcbfm.com

Two binding sites for [^{3}H]PBR28 in human brain: implications for TSPO PET imaging of neuroinflammation

David R Owen[1,3], Owain W Howell[2], Sac-Pham Tang[3], Lisa A Wells[3], Idriss Bennacef[3], Mats Bergstrom[3], Roger N Gunn[3,4], Eugenii A Rabiner[3,4], Martin R Wilkins[1], Richard Reynolds[2], Paul M Matthews[3,4] and Christine A Parker[3]

[1]*Department of Experimental Medicine and Toxicology, Imperial College London, Hammersmith Hospital, London, UK;* [2]*Department of Cellular and Molecular Neuroscience, Imperial College London, Hammersmith Hospital, London, UK;* [3]*Clinical Imaging Centre, GlaxoSmithKline, London, UK;* [4]*Department of Clinical Neuroscience, Imperial College London, Hammersmith Hospital, London, UK*

[^{11}C]PBR28, a radioligand targeting the translocator protein (TSPO), does not produce a specific binding signal in approximately 14% of healthy volunteers. This phenomenon has not been reported for [^{11}C]PK11195, another TSPO radioligand. We measured the specific binding signals with [^{3}H]PK11195 and [^{3}H]PBR28 in brain tissue from 22 donors. Overall, 23% of the samples did not generate a visually detectable specific autoradiographic signal with [^{3}H]PBR28, although all samples showed [^{3}H]PK11195 binding. There was a marked reduction in the affinity of [^{3}H]PBR28 for TSPO in samples with no visible [^{3}H]PBR28 autoradiographic signal ($K_i = 188 \pm 15.6$ nmol/L), relative to those showing normal signal ($K_i = 3.4 \pm 0.5$ nmol/L, $P < 0.001$). Of this latter group, [^{3}H]PBR28 bound with a two-site fit in 40% of cases, with affinities (K_i) of 4.0 ± 2.4 nmol/L (high-affinity site) and 313 ± 77 nmol/L (low-affinity site). There was no difference in K_d or B_{max} for [^{3}H]PK11195 in samples showing no [^{3}H]PBR28 autoradiographic signal relative to those showing normal [^{3}H]PBR28 autoradiographic signal. [^{3}H]PK11195 bound with a single site for all samples. The existence of three different binding patterns with PBR28 (high-affinity binding (46%), low-affinity binding (23%), and two-site binding (31%)) suggests that a reduction in [^{11}C]PBR28 binding may not be interpreted simply as a reduction in TSPO density. The functional significance of differences in binding characteristics warrants further investigation.
Journal of Cerebral Blood Flow & Metabolism (2010) **30,** 1608–1618; doi:10.1038/jcbfm.2010.63; published online 28 April 2010

Keywords: PBR; [^{3}H]PBR28; [^{3}H]PK11195; radioligand binding; TSPO

Introduction

The 18 kDa translocator protein (TSPO), previously known as the peripheral benzodiazepine receptor (PBR), is strongly expressed in microglia and macrophages (Papadopoulos *et al*, 2006). For this reason, the TSPO-targeting positron emission tomography (PET) radioligand, [^{11}C]PK11195, has been applied to studying disease processes that involve microglial activation or the recruitment of macrophages, such as multiple sclerosis (MS), ischaemic stroke, herpes encephalitis, Parkinson's disease, or Alzheimer's disease (Banati *et al*, 2000; Cagnin *et al*, 2001; Edison *et al*, 2008; Gerhard *et al*, 2006; Ramsay *et al*, 1992). The TSPO is an attractive target for this application as it is expressed only at low levels in the healthy human brain (Doble *et al*, 1987). The TSPO exists both as a monomer and as part of a multimeric complex involving several TSPO monomers with associated proteins, including the voltage-dependent anion channel (Boujrad *et al*, 1994, 1996; Rao and Butterworth, 1997). Although subunit interactions are not necessary for drug ligands to bind the TSPO monomer (Joseph-Liauzun *et al*, 1997; Lacapere *et al*, 2001), binding of some drugs to the TSPO is influenced by these interactions (Golani *et al*, 2001).

It is well recognised that *in vivo* PET applications of [^{11}C]PK11195 are limited by the low affinity and low extraction in brain, resulting in poor signal-to-noise ratio (Banati *et al*, 2000). There has therefore been considerable interest in developing improved TSPO

Correspondence: Dr David R Owen, Department of Experimental Medicine and Toxicology, Imperial College London, Hammersmith Hospital, Du Cane Road, London W12 0NN, UK.
E-mail: d.owen@imperial.ac.uk
This research has been supported by GlaxoSmithKline, Imperial College London and The Wellcome Trust.
Received 12 February 2010; revised 24 March 2010; accepted 12 April 2010; published online 28 April 2010

tracers, and various candidate molecules have been generated, including PBR06 (Imaizumi *et al*, 2007), FEPPA (Wilson *et al*, 2008), DAA1106 (Okubo *et al*, 2004), and PBR111 (Fookes *et al*, 2008). This paper explores [11C]PBR28, a new TSPO-targeting PET radioligand, which has a favourable specific-to-nonspecific binding ratio (Imaizumi *et al*, 2008). [11C]PBR28 is displaced by unlabelled PK11195 (Imaizumi *et al*, 2008) and unlabelled PBR28 displaces [3H]PK11195 (Briard *et al*, 2008), but it is not known whether PK11195 and PBR28 bind the same site on the TSPO.

A recent clinical PET study using [11C]PBR28 has reported that 14% of healthy volunteers did not have a specific binding signal in either the brain or the peripheral organs (Fujita *et al*, 2008). The reason for this is not fully understood. Various hypotheses can be entertained, including conformational changes in the TSPO molecule, displacement by endogenous factors, reduction in expression, or pharmacokinetic factors preventing the radiotracer from reaching the TSPO target.

In this paper, we use frozen section autoradiography to confirm the observation of apparent PBR28 nonbinding, and then directly compare the quantitative binding of [3H]PBR28 with that of [3H]PK11195 in human brain tissue *in vitro*.

Materials and methods

Human Tissue

Tissue from donors 1 to 6 inclusive was obtained from the UK National Multiple Sclerosis (MS) Brain Bank for an initial pilot study. Samples from 16 further donors were later obtained from the same source to increase the sample size. Of the 22 donors, 20 had been diagnosed with MS, and 2 were control donors without MS, neuropathological reports for which showed age-related changes only. Initial autoradiography results identified five apparent PBR28 nonbinding subjects. Tissue blocks from these subjects were obtained for quantitative binding studies. We also randomly selected tissue blocks from 10 individuals with apparently normal PBR28 binding to serve as comparisons in these studies.

Tissue Used in Autoradiographical Studies

Tissue blocks were sectioned (10 μm thickness) using a cryostat microtome (Leica, Wetzlar, Germany; CM1900) and thaw-mounted onto superfrost glass microscope slides. Slides were stored at -80°C until use. For donors 1 to 6 inclusive, tissue was sectioned specifically for the study and used within 14 days of sectioning. For the remaining donors, the tissue had been sectioned up to 300 days before use.

Tissue Used in Homogenate and Competition Binding Assays

Tissue blocks contained histopathologically 'normal appearing' tissue, without immunohistochemical evidence of demyelination or significant inflammatory infiltrate. The tissue was stored at -80°C until use.

Demographic, tissue handling, and clinical information regarding the donor is shown in Table 1.

Table 1 Demographic, disease, and tissue-handling details

Donor number	*Sex*	*Age at death (years)*	*Time from death to study (days)*	*Time from death to organ harvesting (hours)*	*Cause of death*	*Disease duration (years)*	*MS diagnosis*
1*	F	42	1709	31	Multiple sclerosis	20	Secondary progressive
2*	F	59	800	21	Bronchopneumonia	39	Secondary progressive
3*	M	66	894	16	Gastrointestinal bleeding	29	Primary progressive
4*	M	88	1304	22	Prostate cancer	NA	Control patient
5*	F	64	3101	7	Gastrointestinal bleed	36	Secondary progressive
6*	M	84	1044	5	Bronchopneumonia	NA	Control patient
7*	F	49	3084	31	Chronic renal failure	18	Secondary progressive
8*	M	54	3045	13	Bronchopneumonia	17	Primary progressive
9*	F	54	2987	22	Bronchopneumonia	20	Secondary progressive
10*	F	39	2726	18	Bronchopneumonia	21	Secondary progressive
11*	M	38	2724	19	Aspiration pneumonia	16	Progressive relapsing
12*	M	40	2487	10	Respiratory failure	12	Secondary progressive
13	F	39	2321	12	Multiple sclerosis	22	Secondary progressive
14	F	44	2315	18	Aspiration pneumonia	16	Secondary progressive
15	F	48	2052	28	Bronchopneumonia	31	Secondary progressive
16	F	51	1988	10	Bronchopneumonia	27	Secondary progressive
17	M	53	1709	13	Bronchopneumonia	16	Secondary progressive
18	M	53	1673	14	Sepsis	33	Secondary progressive
19	F	64	1314	8	Aspiration pneumonia	37	Secondary progressive
20*	F	44	1980	20	Sepsis	19	Secondary progressive
21*	M	46	2821	7	Bronchopneumonia	8	Secondary progressive
22*	F	53	1944	17	Multiple sclerosis	28	Secondary progressive

F, female; M, male; NA, not applicable.
Further tissue was obtained from 15 of the 22 (marked *) for quantitative binding studies.
Numbering of the donors was based on autoradiography results.

Materials

[3H]PK11195 (1-(2-chlorophenyl)-*N*-methyl-*N*-(1-methylpropyl)-3-isoquinolinecarboxamide, specific activity = 80 Ci/mmol; radioactive concentration = 1.0 mCi/mL) was purchased from Perkin Elmer, Cambridge, UK and [3H]PBR28 (*N*-{[2-(methyloxy)phenyl]methyl}-*N*-[4-(phenyloxy)-3-pyridinyl] acetamide; specific activity = 82 Ci/mmol; radioactive concentration = 1.0 mCi/mL) was custom labelled by GE Healthcare, Amersham, UK. Unlabelled PK11195 and PBR28 were purchased from Sigma, Gillingham, UK and Borochem, Caen, France, respectively.

Frozen Section Autoradiography

Initial *in vitro* binding studies were performed using rat tissue and either [3H]PBR28 or [3H]PK11195 to determine the optimal experimental conditions to maximise the ratio of specific-to-nonspecific binding for each radioligand (data not shown).

Autoradiography binding studies were performed on the sectioned human tissue using the optimised experimental conditions. Briefly, sections from each donor were thawed to room temperature (RT) and washed for 15 minutes in assay buffer (50 mmol/L Tris Base, 140 mmol/L NaCl, 1.5 mmol/L $MgCl_2$, 5 mmol/L KCl, 1.5 mmol/L $CaCl_2$, pH 7.4, RT). Sections were incubated in assay buffer containing either [3H]PBR28 (0.5 nmol/L) for 60 minutes or [3H]PK11195 (1 nmol/L) for 120 minutes. The nonspecific binding component was determined on adjacent sections in the presence of unlabelled PK11195 (10 μmol/L). After incubation, slides were washed twice in ice-cold wash buffer (50 mmol/L Tris Base, 1.4 mmol/L $MgCl_2$, pH 7.4, 4°C; 60 seconds) followed by a final wash in ice-cold distilled water (4°C; 60 seconds). Slides were dried in a cool airstream before exposure to tritium-sensitive film (Kodak Biomax MS film, Hemel Hempstead, UK) with [3H]microscale standards (GE Healthcare, Amersham, UK) in X-ray cassettes at RT (4 weeks). After development of the radiograms, the films were quantified using microcomputer imaging device analysis software (Microcomputer Imaging Device Core 7.0; Interfocus Imaging Ltd, Linton, UK). Regions of interest (ROIs) were generated for each area of (unless otherwise stated) nondiseased grey matter on each tissue section. Nondiseased grey matter was defined as an area of grey matter with no microscopic evidence of demyelination or inflammation, as defined by the immunohistochemical stains outlined below. Values were converted to fmol [3H]ligand/mg wet tissue equivalent using the calibrated [3H]microscale standards.

To determine the affinities of [3H]PBR28 and [3H]PK11195 for the TSPO, saturation autoradiography studies were performed for donors 1 to 6 inclusive (this was not possible for donors 7 to 22 inclusive because of insufficient tissue). Seven concentrations of [3H]PBR28 and [3H]PK11195 were used, ranging from 100 pmol/L to 100 nmol/L. The nonspecific binding component was defined by addition of unlabelled PK11195 (10 μmol/L) to adjacent sections. Regions of interests were placed on nondiseased grey matter for autoradiograph quantification unless otherwise stated.

Immunohistochemistry

Sections adjacent to those used for frozen section autoradiography were stained with antibodies to identify microglia/macrophages (CD68 (DAKO, Ely, UK), major histocompatibility complex class II (Abcam, Cambs, UK)), and with antimyelin oligodendrocyte glycoprotein (antibody provided: courtesy of R Reynolds, Imperial College London) to define demyelination. This was performed for donors 1 to 6 inclusive, but was not possible for the remaining donors because of insufficient tissue.

Membrane Preparation

Tissue blocks, obtained from 15 of 22 donors, were homogenised in 10 times weight for volume buffer (0.32 mmol/L sucrose, 5 mmol/L Tris-Base, 1 mmol/L $MgCl_2$, pH 7.4, 4°C). Homogenates were centrifuged ($32{,}000 \times g$, 20 minutes, 4°C) followed by removal of the supernatant. Pellets were resuspended in at least 10 times w/v (weight for volume) buffer (50 mmol/L Tris-Base, 1 mmol/L $MgCl_2$, pH 7.4, 4°C) followed by two washes by centrifugation ($32{,}000 \times g$, 20 minutes, 4°C). Membranes were suspended in buffer (50 mmol/L Tris-Base, 1 mmol/L $MgCl_2$, pH 7.4, 4°C) at a protein concentration of approximately 4 mg protein/mL and aliquots were stored at −80°C until use.

Homogenate and Competition Binding Assays

Aliquots (approximately 250 μg protein/mL) of membrane suspension were prepared using assay buffer (50 mmol/L Tris-Base, 140 mmol/L NaCl, 1.5 mmol/L $MgCl_2$, 5 mmol/L KCl, 1.5 mmol/L $CaCl_2$, pH 7.4, 37°C) and incubated with [3H]PK11195 or [3H]PBR28 at 37°C in a final volume of 500 μL for 60 minutes. For saturation analysis, eight concentrations of either [3H]PK11195 or [3H]PBR28 were used, ranging from 100 pmol/L to 1000 nmol/L. The specific binding component associated for both radioligands was defined by addition of unlabelled PK11195 (10 μmol/L). After incubation, assays were terminated by filtration through Whatman GF/B filters (Whatman, Maidstone, UK), followed by 3×1 mL washes with ice-cold wash buffer (50 mmol/L Tris-Base, 1.4 mmol/L $MgCl_2$, pH 7.4, 4°C). Whatman GF/B filters were preincubated with 0.05% polyethyleneimine (60 minutes) before filtration. Scintillation fluid (3 mL/vial, Perkin Elmer Ultima Gold MV) was added and vials counted on a Perkin Elmer Tricarb 2900 liquid scintillation counter. Each point was performed in triplicate. B_{max} (fmol per mg protein) and K_d (nmol/L) values were determined using GraphPad Prism 5.0 software (GraphPad Software Inc., La Jolla, CA, USA).

Competition assays were performed under the same conditions as the homogenate binding assays above. Each assay well contained [3H]PK11195 (4 nmol/L) with unlabelled PK11195 (10 concentrations ranging from 0.1 nmol/L to 3 μmol/L) or unlabelled PBR28 (12 concentrations ranging from 0.1 nmol/L to 30 μmol/L). The specific binding component was determined using unlabelled PK11195 (10 μmol/L). For each donor, each point was performed in triplicate, except for the total and nonspecific wells that were performed in sextuplicate.

Protein Concentration Determination

Protein concentrations (μg protein/mL) were determined using the bicinchoninic acid assay (BCA Kit, Sigma-Aldrich, Gillingham, UK) and absorption read at 562 nm.

Data Analysis

All saturation and competition data were analysed using the iterative nonlinear regression curve-fitting software supplied with GraphPad Prism 5.0. Single-site and two-site models were compared using the least-squares algorithm. The null hypothesis, that the data fitted a single-site model, was rejected if the *P*-value was less than 0.05. The mean K_d value for [3H]PK11195 was used to generate the K_i for unlabelled PBR28 and PK11195. Autoradiography tissue ROIs were quantified on the total sections and ROIs were aligned with the adjacent nonspecific binding section, to determine the specific binding component. All data were analysed independently and are expressed as the mean ± s.d. Student's *t*-test (GraphPad Prism) was used to determine the statistical significance.

Results

Localisation of Binding—Frozen Section Autoradiography

All six donors in the pilot study produced a specific binding signal with [3H]PK11195 in both grey and white matter. The specific binding signal associated with [3H]PK11195 in normal grey matter was higher than in normal white matter, allowing the two to be clearly distinguished by visual inspection (Figure 1). In donors with MS, there were also well-defined areas of high specific binding within the white matter, consistent with the expected shape, size, and distribution of the inflammatory lesions characteristic of MS. For four of the six brains [3H]PBR28-specific binding colocalised with [3H]PK11195-specific binding and binding was greater in the grey relative to the white matter. However, for two of the six brains (donors 5 and 6) no apparent specific binding associated with [3H]PBR28 was identified (Figure 1). The specific signal for these two donors with [3H]PK11195 was comparable to that for sections from other donors (Figure 1 and Supplementary Table). These two donors did not differ from others with regard to demographics or disease expression (Table 1).

Tissue from all six donors was examined using immunohistochemistry. In two of the six donors who were healthy controls without MS, immunohistochemistry revealed no pathology. In three of the

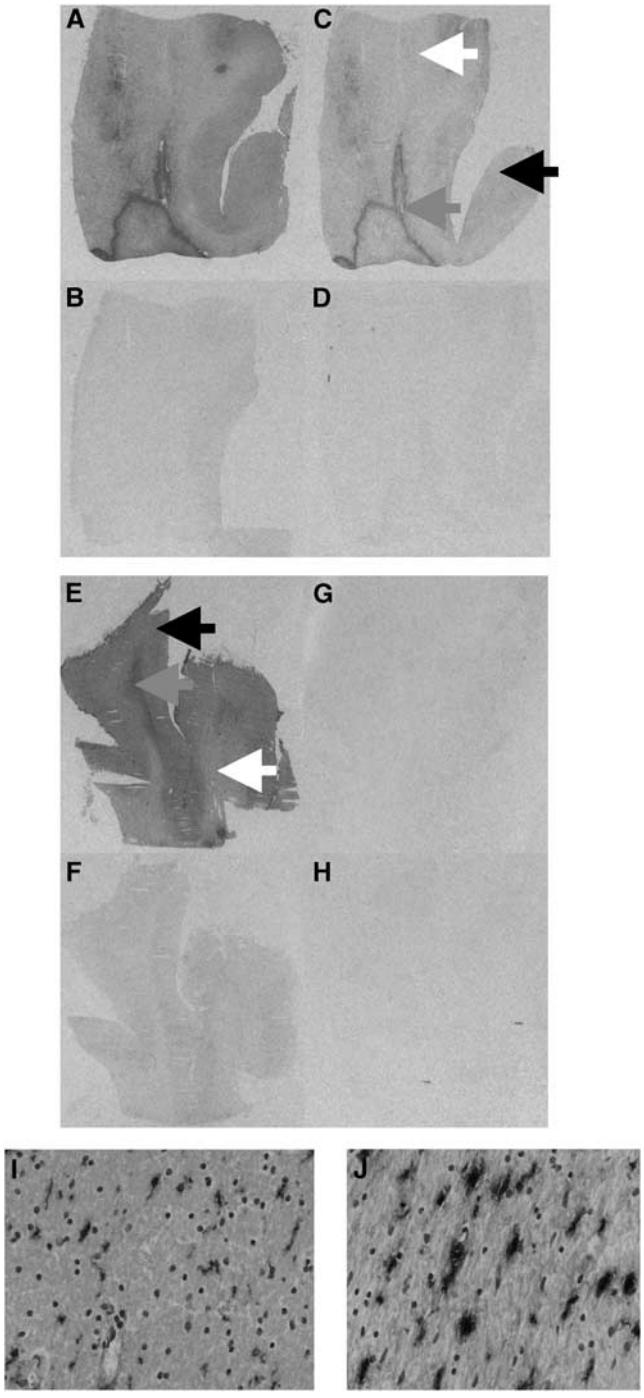

Figure 1 Representative images for total and nonspecific binding in a high affinity binder (Donor 1) and a low-affinity binder (Donor 5) with [3H]PBR28 and [3H]PK11195, and colocalisation of [3H]PK11195 binding with major histocompatibility complex class II (MHC II) staining in a low-affinity binder (Donor 5). (**A**, **B**) Donor 1 [3H]PK11195 total binding and nonspecific binding, (**C**, **D**) donor 1 [3H]PBR28 total binding and nonspecific binding; (**E**, **F**) donor 5 [3H]PK11195 total binding and nonspecific binding; (**G**, **H**) donor 5 [3H]PBR28 total binding and nonspecific binding. (**I**) Low MHC II expression from normal appearing white matter (× 400 magnification) colocalising with low [3H]PK11195 binding; (**J**) high MHC II expression from white matter lesion (× 400 magnification) corresponding with high [3H]PK11195 binding. Normal white matter is represented by the white arrow; normal grey matter by the black arrow; and white matter lesion by the red arrow.

remaining four donors (all of whom had an antemortem diagnosis of MS), immunohistochemistry showed that the well-defined areas of high-specific binding (seen with both [3H]PK11195 and [3H]PBR28) were white matter inflammatory lesions with high expression of the microglia/macrophage markers major histocompatibility complex class II and CD68. Tissue from the fourth donor with MS (donor 5, who had no visible signal with [3H]PBR28) showed well-defined areas of high [3H]PK11195-specific binding colocalising with high expression of major histocompatibility complex class II and CD68 (Figure 1).

To estimate the relative incidence of apparent nonbinding with [3H]PBR28, tissue from 16 further donors was used. Although experimental conditions were kept identical, this tissue had been sectioned up to 300 days before use (in contrast to tissue from donors 1 to 6, which had been sectioned within 14 days of use). All sections used in this group produced a specific signal with [3H]PK11195 that was greater in grey matter than in white matter.

A similar pattern of higher binding to grey matter was observed with [3H]PBR28 for 13 of the 16 brains in this group. However, for three cases (donors 20, 21, and 22) there was no visible binding associated with [3H]PBR28. Nonetheless, similar to the findings with donors 1 to 6, [3H]PK11195-specific binding for these three cases was no different from that for the rest of the group (Supplementary Table). Furthermore, as with donors 1 to 6, the cases with no visible binding did not differ in demography from the rest of group (Table 1).

When tissue sections for the two donor groups (donors 1 to 6 and donors 7 to 22) were compared, donors 1 to 6 showed fivefold greater [3H]PK11195-specific binding than donors 7 to 22 (206.7 ± 15.4 versus 43.4 ± 20.4 fmol per mg of protein, $P < 0.0001$). No significant differences between the two groups were observed for [3H]PBR28 (96.0 ± 2.4 versus 149.5 ± 81.67 fmol per mg of protein, $P = 0.30$).

Estimation of K_d—Autoradiography Saturation Studies

To determine whether the sections with no visible binding with [3H]PBR28 had a reduced affinity for this radioligand relative to sections from the other donors, the affinities for both [3H]PBR28 and [3H]PK11195 were measured using tissue sections from donors 1 to 6. No significant difference in K_d for [3H]PK11195 was found for those cases with no visible [3H]PBR28 signal (1.5 ± 1.60 nmol/L) relative to the rest of the group (2.2 ± 0.90 nmol/L, $P = 0.51$). However, there was an approximate 16-fold reduction in affinity for [3H]PBR28 in cases with no visible binding (15.8 ± 2.658 nmol/L), hereafter referred to as low-affinity binders (LABs), relative to the rest of the group (1.0 ± 0.47 nmol/L, $P = 0.0003$), hereafter referred to as high-affinity binders (HABs). K_d values obtained from ROIs confined to either normal white matter or white matter lesions did not differ from those obtained using ROIs confined to grey matter (data not shown).

Estimation of B_{max} and K_d—Homogenate Saturation Binding Studies

To better estimate the binding affinities and apparent expression levels of the TSPO in HABs and LABs, the K_d and density of available binding sites (B_{max}) for the two radioligands were determined using tissue homogenates generated from brain tissue originating from 15 of the 22 donors. This group included all five LABs identified by autoradiography and 10 HABs (Table 1). Data obtained with [3H]PK11195 fitted well to a single-site model for all assays. However, with [3H]PBR28, while data from 11 of the 15 donors fitted to a single-site model, the data fitted best to a two-site model in assays for the remaining four donors (all of whom were HABs).

For [3H]PK11195, there was no significant difference in data obtained from assays with tissue from LABs in either K_d (30.6 ± 13.7 nmol/L) or B_{max} (5063 ± 1313 fmol per mg protein) relative to the HABs (K_d 28.5 ± 14.4 nmol/L and B_{max} 4325 ± 1540 fmol per mg protein) (K_d $P = 0.79$; B_{max} $P = 0.38$) Figures 2A and 2C; Table 2).

The affinity for [3H]PBR28 in samples from LABs (52.4 ± 23.1 nmol/L) was approximately 25 times lower than that obtained with HABs (2.2 ± 0.48 nmol/L) ($P < 0.001$) (Figure 2B, Table 2). For the four donors (all HABs) for which a best fit was found with a two-site model, the mean K_d for the high- and low-affinity sites were 1.3 ± 0.2 and 135 ± 161 nmol/L, respectively. Hereafter, we refer to this group (a subset of HABs) as mixed-affinity binders (MABs).

The B_{max} for LABs (994 ± 353 fmol per mg protein) was lower than that obtained for HABs (1929 ± 657 fmol per mg protein, $P = 0.02$) (Figure 2D, Table 2). B_{max} was significantly greater when using [3H]PK11195 compared with that when using [3H]PBR28. This difference was consistently shown in tissues from all 15 donors used in these quantitative studies. The mean density of [3H]PBR28 binding sites was approximately one-third of that obtained with [3H]PK11195 (Table 2).

Estimation of K_i—Competition Binding Studies

To accurately assess binding at the low-affinity site for [3H]PBR28 in tissue from the four MABs, high concentrations of radioligand would be required and self-block would be a concern, because only a small fraction of the ligand is successfully labelled. Competition binding assays were therefore performed. Results from these assays consistently fitted to a single-site model for PK11195, with K_i values that were not significantly different between HABs (26.4 ± 10.0 nmol/L) and LABs (22.3 ± 4.9 nmol/L) ($P = 0.41$) (Table 3, Figure 3A).

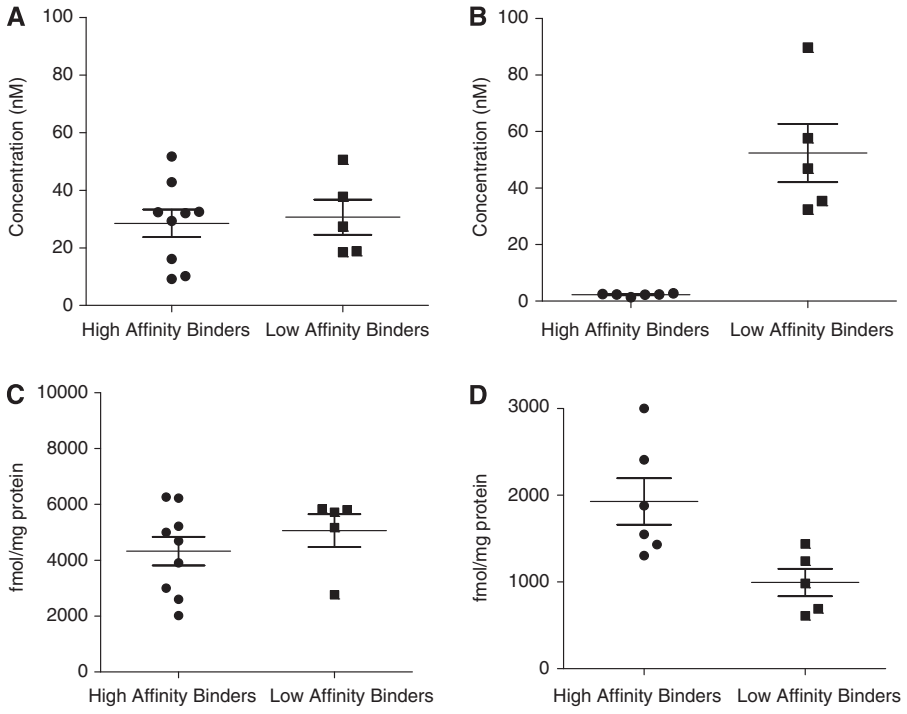

Figure 2 K_d and B_{max} for [3H]PK11195 and [3H]PBR28. (**A**) K_d for [3H]PK11195, (**B**) K_d for [3H]PBR28, (**C**) B_{max} for [3H]PK11195, (**D**) B_{max} for [3H]PBR28. Where data fitted a two-site fit, the K_d for the high-affinity site and the total B_{max} (for both high- and low-affinity sites) were used to calculate means.

Table 2 Homogenate binding studies: B_{max} and K_d for HABs and LABs with [3H]PBR28 and [3H]PK11195

Donor	*[3H]PK11195: K_d (nmol/L) and B_{max} (fmol per mg protein)*		*[3H]PBR28: K_d (nmol/L) and B_{max} (fmol per mg protein) using a single-site model*		*[3H]PBR28: K_d (nmol/L) and B_{max} (fmol per mg protein) for two-site model, where appropriate*		
	B_{max}	K_d	B_{max}	K_d	*Total B_{max} (for both sites)*	*k_d (High-affinity site)*	*K_d (Low-affinity site)*
HABs							
1	4998	16.17	1432	2.49			
2	6223	32.39	2410	2.23			
3	3003	29.36	1550	2.75			
4	3908	51.72	1305	1.34			
7	6263	42.79	1879	2.30			
8	5217	32.03	1296[a]	2.22[a]	1479	1.1	21
9	4693	32.51	977[a]	2.35[a]	2337	1.48	374
10	[b]	[b]	3000	2.36			
11	2599	10.18	1199[a]	3.53[a]	1709	1.48	69
12	2018	9.23	1305[a]	2.86[a]	1917	1.15	76
Mean ± s.d.	4325 ± 1540 (n = 9)	28.5 ± 14.35 (n = 9)	1929 ± 657 (n = 6)	2.2 ± 0.48 (n = 6)	1861 ± 365 (n = 4)	1.3 ± 0.2 (n = 4)	135 ± 161 (n = 4)
LABs							
5	5843	27.44	1440	35.36			
6	2765	18.53	611	32.42			
20	5725	50.59	691	46.85			
21	5174	18.83	985	89.64			
22	5808	37.79	1243	57.58			
Mean ± s.d.	5063 ± 1313 (n = 5)	30.6 ± 13.65 (n = 5)	994 ± 353 (n = 5)	52.4 ± 23.13 (n = 5)			
T-test	P = 0.38	P = 0.79	P = 0.02	P < 0.001			

HABs, high-affinity binders; LABs, low-affinity binders.

[a]Data did not fit a single-site model and was therefore excluded from calculation of mean B_{max} and K_d.

[b]Curve did not reach full plateau, and therefore accurate values for K_d and B_{max} could not be calculated.

Table 3 Competition binding studies: K_i for HABs and LABs with PK11195 and PBR28

Donor number	*Ki (nmol/L) of PK11195*	*Ki (nmol/L) of PBR28 using single-site fit*	*Ki (nmol/L) of PBR28 for both binding sites in which data fitted fit model*		
			High-affinity site	*Low-affinity site*	*Fraction of high-affinity sites*
HABs					
1	39.4	4.4			
2	15.3	3.3			
3	22.2	3.0			
4	40.0	3.6			
7	23.8	3.0			
8	15.7	27.3[a]	4.1	310	0.55
9	38.6	43.7[a]	7.1	313	0.52
10	28.9	3.1			
11	24.6	55.3[a]	1.3	221	0.41
12	15.3	22.4[a]	3.3	409	0.58
Mean ± s.d.	26.4 ± 10.0 (n = 10)	3.4 ± 0.5 (n = 6)	4.0 ± 2.4 (n = 4)	313 ± 76.8 (n = 4)	0.52 ± 0.07 (n = 4)
LABs					
5	21.8	178.4			
6	28.3	194.9			
20	24.7	194.1			
21	21.7	206.4			
22	15.0	166.7			
Mean ± s.d.	22.3 ± 4.9 (n = 5)	188 ± 15.6 (n = 5)			
T-test (HABs versus LABs)	P = 0.41	P < 0.0001			

HABs, high-affinity binders; LABs, low-affinity binders.
[a]Data did not fit a single-site model and was therefore excluded from calculation of mean K_i.

Competition assays using unlabelled PBR28 confirmed a single-site best fit in tissue from the 11 donors who had previously shown a single-site fit in [3H]PBR28 saturation studies. The difference in affinity for HABs (K_i 3.40 ± 0.5 nmol/L) and LABs (K_i 188 ± 15.6 nmol/L) was consistent with saturation studies (Table 3).

Competition data also confirmed the two-site fit for the four MABs who had previously shown a two-site fit in the saturation study with [3H]PBR28 (Figure 3B). The mean K_i for the MAB low-affinity binding site from the competition assays was 313 nmol/L, and the confidence intervals for this estimate (191 to 435 nmol/L) overlapped with the confidence intervals for the estimate of the LAB site (169 to 207 nmol/L). This raises the possibilities that (1) the LAB site and the lower-affinity MAB site may be the same site, and, if so, (2) MABs may express both a HAB and an LAB site. To investigate these hypotheses, we fitted the data from the competition assays to the equations below, which assume that MABs have an equal number of high- and low-affinity binding sites (Figure 3B). When fitted in this manner, the affinities for the high- and low-affinity sites were estimated to be 5.4 and 172 nmol/L, respectively. We explored the data further and removed the constraint fixing the two sites to a 50:50 distribution. This analysis suggested that the two sites were distributed at 43:57 (high/low) with affinities of 4.6 and 145 nmol/L, respectively.

HABs:

$$\mathrm{SP} = (1 - \mathrm{NS})\frac{K_i^{\mathrm{H}}}{K_i^{\mathrm{H}} + [\mathrm{PBR28}]} + \mathrm{NS}$$

LABs:

$$\mathrm{SP} = (1 - \mathrm{NS})\frac{K_i^{\mathrm{L}}}{K_i^{\mathrm{L}} + [\mathrm{PBR28}]} + \mathrm{NS}$$

MABs:

$$\mathrm{SP} = (1 - \mathrm{NS})\left[\frac{f_{\mathrm{H}}K_i^{\mathrm{H}}}{K_i^{\mathrm{H}} + [\mathrm{PBR28}]} + \frac{(1 - f_{\mathrm{H}})K_i^{\mathrm{L}}}{K_i^{\mathrm{L}} + [\mathrm{PBR28}]}\right] + \mathrm{NS}$$

where SP is the specific binding of [3H]PK11195; NS, nonspecific binding; and f_{H}, the fraction of high-affinity binding sites.

Discussion

We have compared the binding characteristics of the novel TSPO ligand, PBR28, with the those of the previously characterised TSPO radioligand, PK11195 (Doble *et al*, 1987), in tissue from human brain. Autoradiography revealed that tissue from 5 of the 22 donors (23%) did not show a measurable binding signal after incubation with [3H]PBR28 at a concentration close to the reported K_i of 2.5 nmol/L

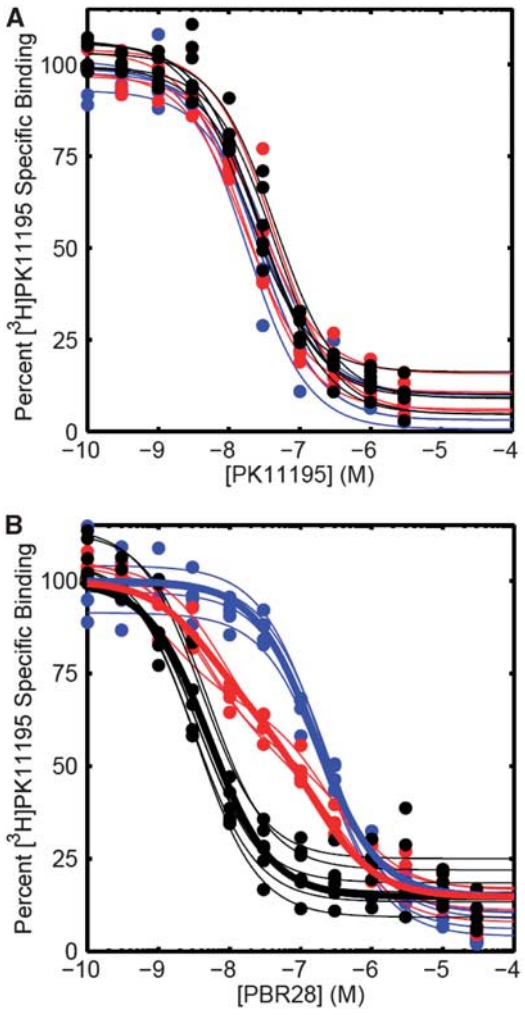

Figure 3 (**A**) Competition assay with [3H]PK11195 in the presence of increasing concentrations of unlabelled PK11195. Curves show individual fits to each subject's data. The nonspecific binding has been subtracted to leave the specific binding, which has been normalised to 100% specific binding. Blue—low-affinity binder (LAB). Black—high-affinity binder (HAB). Red—mixed-affinity binder (MAB). (**B**) Competition assay with [3H]PK11195 in the presence of increasing concentrations of unlabelled PBR28. Thin lines show individual fits to each subject's data. Thick lines show results from the population fit defined by the equations in the text, which assume that MABs have both HAB and LAB binding sites (percentage of each unspecified). The nonspecific binding has been subtracted to leave the specific binding, which has been normalised to 100% specific binding. Blue—low-affinity binder (LAB). Black—high-affinity binder (HAB). Red—mixed-affinity binder (MAB).

(Briard *et al*, 2008). In contrast, [3H]PK11195 binding in these sections did not differ from that measured in tissue sections from other donors showing strong [3H]PBR28 binding. Preserved [3H]PK11195 binding in the expected distribution (Doble *et al*, 1987) across grey matter, white matter, and inflammatory lesions further confirmed that the TSPO was present in tissue that did not appear to bind [3H]PBR28. Our observation that 23% of the donors did not have a visible [3H]PBR28 signal is comparable to the case of the 14% of volunteers who were reported by Fujita *et al* (2008) to not have a specific PET signal.

To more rigorously test the hypothesis that the lack of a measurable [3H]PBR28 signal in 23% of the donors was the result of a reduction in affinity of the TSPO for [3H]PBR28, saturation homogenate and autoradiographical binding studies were performed. Homogenate studies confirmed that those donors with no visible signal had a 25-fold reduction in affinity for [3H]PBR28 compared with the rest of the cohort. Autoradiographical saturation studies using [3H]PBR28 also showed a marked decrease in affinity, which was similar in magnitude to that observed in the homogenate saturation studies. The affinity of [3H]PK11195 for the TSPO was the same for all donors and this radioligand was not able to distinguish the groups in either the homogenate or the autoradiographical studies. We thus can reject the hypothesis that the absence of PBR28-specific binding is because of an absence of TSPO, and propose classifying subjects as LABs or HABs, consistent with results from a recent report showing a reduction in PBR28 affinity in lymphocytes from volunteers who showed no specific [11C]PBR28 signal with PET (Kreisl *et al*, 2010).

The density of TSPO binding sites for [3H]PK11195 was similar for all subjects. In contrast, the density of TSPO binding sites exhibited by [3H]PBR28 was lower for the LABs relative to the HABs. This result must be interpreted with caution, because our sample size is limited. However, we hypothesise that a true difference in B_{max} between HABs and LABs may exist, possibly as a consequence of differences in TSPO or interactions with associated proteins arising from the structural or functional changes responsible for the difference in affinities.

Although one report has speculated that PK11195 may have a low-affinity binding site (Broaddus and Bennett, 1990), the majority of literature published earlier (Doble *et al*, 1987; Miyazawa *et al*, 1998; Rao and Butterworth, 1997; Venneti *et al*, 2008) found evidence for only a single site. Our study supports this conclusion. However, our saturation studies revealed a subgroup (4 of the 10 HABs) with two distinguishable PBR28 binding sites that we label as MABs. Competition binding assays confirmed this. We estimated the K_i for the MAB low-affinity site (313 nmol/L) as being similar to the K_i of the LAB site (188 nmol/L), and the K_i for the MAB high-affinity site (4.0 nmol/L) as being similar to the K_i of the HAB site (3.4 nmol/L). Given the two MAB sites are represented in approximately equal proportion, we speculate that the MABs are heterozygotes for a codominantly expressed binding site, whereas HABs and LABs are homozygotes for alternative forms. This is consistent with our modelling data, which estimated the two binding sites to have affinities of 4.6 and 145 nmol/L, respectively, with a distribution approximating 50:50.

For an allele frequency to be broadly consistent with the proportions of HABs (46%), MABs (31%), and LABs (23%) in the general population, predicted by our enriched sample, it would need to be distributed in the population in a ratio of approximately 2:3 (HAB allele) to 1:3 (LAB allele). However, the known single-nucleotide polymorphisms of the gene encoding the TSPO, His162Arg and Ala147Thr, have distributions of 79:21 and 98:2, respectively (Kurumaji *et al*, 2000). Nevertheless, this does not exclude the possibility that a single-nucleotide polymorphism underlies the different binding states, because our sample is comprised mainly of patients with MS. If MS is associated with either of the two known single-nucleotide polymorphisms, then the single-nucleotide polymorphism distribution in our sample may differ from that in the general population. Similar work is required with control brains to determine whether the MAB state is detected, and if so the relative frequencies of HABs, MABs, and LABs.

The presence of differing affinity profiles is problematic for the interpretation of PET data, as differences in the binding parameters of [^{11}C]PBR28 cannot be assumed to reflect differences in the density of TSPO. Regardless of which measure of binding potential is calculated, for a given receptor density the binding potential will be in the ratio of 55:28:1 for HABs, MABs, and LABs, respectively (assuming that MABs express equal numbers of HAB and LAB sites, which have affinities of 3.4 and 188 nmol/L, respectively). As LABs are easily identifiable and therefore easily eliminated from a cohort, it will be difficult to differentiate MABs with an elevated TSPO density from HABs in whom TSPO density is normal. Assuming binding status remains constant over time, intra-patient comparisons required to measure the effect of treatment or disease progression may still be feasible. Assuming that binding status is consistent across different tissues (centrally and peripherally), inter-patient comparisons would also still be feasible by classifying the subjects into groups (HABs, MABs, or LABs) on the basis of binding assays of peripheral blood cells. In theory, population corrections could then be applied to compare subjects in different binding groups. Although early evidence suggests that LAB and HAB status may remain constant over time and across tissue (Kreisl *et al*, 2009), it is important to definitively show this for all three binding groups.

Preserved [^{3}H]PK11195 binding in LABs suggests that there are two distinct TSPO binding sites, one binding PK11195 and a second (with two forms) binding PBR28. Additional observations were consistent with this. B_{max} values obtained with [^{3}H]PK11195 in the homogenate binding study were consistently higher (by a mean of threefold) than those obtained with [^{3}H]PBR28. Similar differences in B_{max} between PK11195 and Ro5-4864 (a benzodiazepine with high affinity for the TSPO) have also been reported in humans (Rao and Butterworth, 1997), rat, guinea pig, cat, and calf (Awad and Gavish, 1989). Tissue handling influenced autoradiography binding of the two radioligands in different ways. The specific signal from [^{3}H]PK11195 was significantly lower in tissue sections that had been stored long term, compared with the tissue that had been stored as a tissue block and sectioned just before use. However, no significant differences were observed with [^{3}H]PBR28 between the two groups. In separate pilot experiments conducted before those reported here, we also observed that fixation with paraformaldehyde markedly reduces PBR28 binding but has no discernable effect on PK11195 binding (data not shown).

Our conclusion that there are distinct binding sites for the two radioligands has precedent. Ro5-4864 shows a two-site fit in the cerebral cortex of rat, mouse, guinea pig, rabbit, and calf (Awad and Gavish, 1987, 1989; Eshleman and Murray, 1989), as well as rat and calf kidney (Awad and Gavish, 1989). A second site is expressed transiently in a murine Leydig cell line after stimulation with human chorionic gonadotropin (Boujrad *et al*, 1994). However, in an earlier study using human brain tissue from six donors, a second site was not reported (Rao and Butterworth, 1997).

It was previously suggested that PK11195 binds the TSPO itself, whereas Ro5-4864 (although it can bind the isolated TSPO) binds only one TSPO molecule within the multimeric functional complex (Rao and Butterworth, 1997), which is formed by clusters of four to six TSPO molecules associated with proteins, including the voltage-dependant anion channel (Boujrad *et al*, 1994, 1996; Rao and Butterworth, 1997). This model is consistent with the lower B_{max} for Ro5-4864 and the observation that the voltage-dependant anion channel enhances Ro5-4864 binding but has no effect on PK11195 binding (Lacapere *et al*, 2001). We speculate that, similar to Ro5-4864, PBR28 binds only a fraction of TSPO molecules within the multimeric complex. PBR28 binding may displace PK11195 by causing a conformational change transmitted allosterically across the TSPO binding site. Further studies are required to test this hypothesis.

We appreciate that the B_{max} and K_d values we report using [^{3}H]PK11195 on the control and MS donor tissue are higher than those in previous reports published (Doble *et al*, 1987; Miyazawa *et al*, 1998; Rao and Butterworth, 1997; Venneti *et al*, 2008). However, previous pharmacological assays were performed almost exclusively at 4°C or RT, whereas our assays were performed at 37°C (to generate data that are potentially more readily related to *in vivo* PET data). It is not unusual or unexpected for temperature to affect the binding properties of radioligands (Hall *et al*, 1988, 1990). Our autoradiography studies, which were performed at RT, produced K_d values very similar to those reported previously (Doble *et al*, 1987; Miyazawa *et al*, 1998; Rao and Butterworth, 1997; Venneti *et al*, 2008).

We thus have shown that PBR28 binding to human brain tissue can be described as high-affinity binding with a single site (HAB), low-affinity binding with a single site (LAB), or MAB with one high- and one low-affinity site (MAB). In contrast, PK11195 appears to bind only in one way and shows similar affinity in all individuals. We therefore conclude that a difference in [11C]PBR28 binding between subjects cannot be interpreted simply as a difference in TSPO density.

Acknowledgements

The authors thank the UK Multiple Sclerosis Tissue Bank (Director, Prof Richard Reynolds) for providing all human tissue used in this study.

Conflict of interest

The authors declare no conflict of interest.

References

Awad M, Gavish M (1987) Binding of [3H]Ro 5-4864 and [3H]PK 11195 to cerebral cortex and peripheral tissues of various species: species differences and heterogeneity in peripheral benzodiazepine binding sites. *J Neurochem* 49:1407–14

Awad M, Gavish M (1989) Species differences and heterogeneity of solubilized peripheral-type benzodiazepine binding sites. *Biochem Pharmacol* 38:3843–9

Banati RB, Newcombe J, Gunn RN, Cagnin A, Turkheimer F, Heppner F, Price G, Wegner F, Giovannoni G, Miller DH, Perkin GD, Smith T, Hewson AK, Bydder G, Kreutzberg GW, Jones T, Cuzner ML, Myers R (2000) The peripheral benzodiazepine binding site in the brain in multiple sclerosis: quantitative *in vivo* imaging of microglia as a measure of disease activity. *Brain* 123(Part 11):2321–37

Boujrad N, Gaillard JL, Garnier M, Papadopoulos V (1994) Acute action of choriogonadotropin on Leydig tumor cells: induction of a higher affinity benzodiazepine-binding site related to steroid biosynthesis. *Endocrinology* 135:1576–83

Boujrad N, Vidic B, Papadopoulos V (1996) Acute action of choriogonadotropin on Leydig tumor cells: changes in the topography of the mitochondrial peripheral-type benzodiazepine receptor. *Endocrinology* 137:5727–30

Briard E, Zoghbi SS, Imaizumi M, Gourley JP, Shetty HU, Hong J, Cropley V, Fujita M, Innis RB, Pike VW (2008) Synthesis and evaluation in monkey of two sensitive 11C-labeled aryloxyanilide ligands for imaging brain peripheral benzodiazepine receptors *in vivo*. *J Med Chem* 51:17–30

Broaddus WC, Bennett Jr JP (1990) Peripheral-type benzodiazepine receptors in human glioblastomas: pharmacologic characterization and photoaffinity labeling of ligand recognition site. *Brain Res* 518:199–208

Cagnin A, Myers R, Gunn RN, Lawrence AD, Stevens T, Kreutzberg GW, Jones T, Banati RB (2001) *In vivo* visualization of activated glia by [11C] (R)-PK11195-PET following herpes encephalitis reveals projected neuronal damage beyond the primary focal lesion. *Brain* 124(Part 10):2014–27

Doble A, Malgouris C, Daniel M, Daniel N, Imbault F, Basbaum A, Uzan A, Gueremy C, Le FG (1987) Labelling of peripheral-type benzodiazepine binding sites in human brain with [3H]PK 11195: anatomical and subcellular distribution. *Brain Res Bull* 18:49–61

Edison P, Archer HA, Gerhard A, Hinz R, Pavese N, Turkheimer FE, Hammers A, Tai YF, Fox N, Kennedy A, Rossor M, Brooks DJ (2008) Microglia, amyloid, and cognition in Alzheimer's disease: An [11C](R)PK11195-PET and [11C]PIB-PET study. *Neurobiol Dis* 32:412–9

Eshleman AJ, Murray TF (1989) Differential binding properties of the peripheral-type benzodiazepine ligands [3H]PK 11195 and [3H]Ro 5-4864 in trout and mouse brain membranes. *J Neurochem* 53:494–502

Fookes CJ, Pham TQ, Mattner F, Greguric I, Loc'h C, Liu X, Berghofer P, Shepherd R, Gregoire MC, Katsifis A (2008) Synthesis and biological evaluation of substituted [18F]imidazo[1,2-a]pyridines and [18F]pyrazolo [1,5-a]pyrimidines for the study of the peripheral benzodiazepine receptor using positron emission tomography. *J Med Chem* 51:3700–12

Fujita M, Imaizumi M, Zoghbi SS, Fujimura Y, Farris AG, Suhara T, Hong J, Pike VW, Innis RB (2008) Kinetic analysis in healthy humans of a novel positron emission tomography radioligand to image the peripheral benzodiazepine receptor, a potential biomarker for inflammation. *Neuroimage* 40:43–52

Gerhard A, Pavese N, Hotton G, Turkheimer F, Es M, Hammers A, Eggert K, Oertel W, Banati RB, Brooks DJ (2006) *In vivo* imaging of microglial activation with [11C](R)-PK11195 PET in idiopathic Parkinson's disease. *Neurobiol Dis* 21:404–12

Golani I, Weizman A, Leschiner S, Spanier I, Eckstein N, Limor R, Yanai J, Maaser K, Scherubl H, Weisinger G, Gavish M (2001) Hormonal regulation of peripheral benzodiazepine receptor binding properties is mediated by subunit interaction. *Biochemistry* 40:10213–22

Hall H, Wedel I, Halldin C, Kopp J, Farde L (1990) Comparison of the *in vitro* receptor binding properties of N-[3H]methylspiperone and [3H]raclopride to rat and human brain membranes. *J Neurochem* 55:2048–57

Hall H, Wedel I, Sallemark M (1988) Effects of temperature on the *in vitro* binding of 3H-raclopride to rat striatal dopamine-D2 receptors. *Pharmacol Toxicol* 63:118–21

Imaizumi M, Briard E, Zoghbi SS, Gourley JP, Hong J, Fujimura Y, Pike VW, Innis RB, Fujita M (2008) Brain and whole-body imaging in nonhuman primates of [11C]PBR28, a promising PET radioligand for peripheral benzodiazepine receptors. *Neuroimage* 39:1289–98

Imaizumi M, Briard E, Zoghbi SS, Gourley JP, Hong J, Musachio JL, Gladding R, Pike VW, Innis RB, Fujita M (2007) Kinetic evaluation in nonhuman primates of two new PET ligands for peripheral benzodiazepine receptors in brain. *Synapse* 61:595–605

Joseph-Liauzun E, Farges R, Delmas P, Ferrara P, Loison G (1997) The Mr 18,000 subunit of the peripheral-type benzodiazepine receptor exhibits both benzodiazepine and isoquinoline carboxamide binding sites in the absence of the voltage-dependent anion channel or of the adenine nucleotide carrier. *J Biol Chem* 272:28102–6

Kreisl WC, Fujita M, Fujimura Y, Kimura N, Jenko KJ, Kannan P, Hong J, Morse CL, Zoghbi SS, Gladding RL, Jacobson S, Oh U, Pike VW, Innis RB (2010) Comparison of [(11)C]-(R)-PK 11195 and [(11)C]PBR28, two radioligands for translocator protein (18 kDa) in human

and monkey: Implications for positron emission tomographic imaging of this inflammation biomarker. *Neuroimage* 49:2924–32

Kurumaji A, Nomoto H, Yoshikawa T, Okubo Y, Toru M (2000) An association study between two missense variations of the benzodiazepine receptor (peripheral) gene and schizophrenia in a Japanese sample. *J Neural Transm* 107:491–500

Lacapere JJ, Delavoie F, Li H, Peranzi G, Maccario J, Papadopoulos V, Vidic B (2001) Structural and functional study of reconstituted peripheral benzodiazepine receptor. *Biochem Biophys Res Commun* 284:536–41

Miyazawa N, Hamel E, Diksic M (1998) Assessment of the peripheral benzodiazepine receptors in human gliomas by two methods. *J Neurooncol* 38:19–26

Okubo T, Yoshikawa R, Chaki S, Okuyama S, Nakazato A (2004) Design, synthesis and structure-affinity relationships of aryloxyanilide derivatives as novel peripheral benzodiazepine receptor ligands. *Bioorg Med Chem* 12:423–38

Papadopoulos V, Baraldi M, Guilarte TR, Knudsen TB, Lacapere JJ, Lindemann P, Norenberg MD, Nutt D, Weizman A, Zhang MR, Gavish M (2006) Translocator protein (18 kDa): new nomenclature for the peripheral-type benzodiazepine receptor based on its structure and molecular function. *Trends Pharmacol Sci* 27: 402–9

Ramsay SC, Weiller C, Myers R, Cremer JE, Luthra SK, Lammertsma AA, Frackowiak RS (1992) Monitoring by PET of macrophage accumulation in brain after ischaemic stroke. *Lancet* 339:1054–5

Rao VL, Butterworth RF (1997) Characterization of binding sites for the omega3 receptor ligands [3H]PK11195 and [3H]RO5-4864 in human brain. *Eur J Pharmacol* 340:89–99

Venneti S, Wang G, Nguyen J, Wiley CA (2008) The positron emission tomography ligand DAA1106 binds with high affinity to activated microglia in human neurological disorders. *J Neuropathol Exp Neurol* 67:1001–10

Wilson AA, Garcia A, Parkes J, McCormick P, Stephenson KA, Houle S, Vasdev N (2008) Radiosynthesis and initial evaluation of [18F]-FEPPA for PET imaging of peripheral benzodiazepine receptors. *Nucl Med Biol* 35:305–14

Supplementary Information accompanies the paper on the Journal of Cerebral Blood Flow & Metabolism website (http://www.nature.com/jcbfm)